

Aseismic crustal deformation in southwestern Taiwan: Insights into the driving mechanisms

*Kotaro Tsukahara¹, Youichiro Takada¹

1. Graduate school of science Hokkaido University

We have reported aseismic crustal deformation detected by InSAR and GNSS in southwestern Taiwan (Tsukahara and Takada, 2017 JPGU). We used GNSS velocity field to remove the long wavelength noise included in each interferogram. In this presentation, we report the aseismic movement in more detail to gain some insights into the driving mechanism of this rapid and aseismic deformation.

We created six interferograms for ascending orbit and one for descending orbit. For ascending images, we selected the interferometric pairs spanning ~2.5 year to reduce the effects of orbit shifts of ALOS. All interferograms are independent each other. We removed height-dependent phase change by DEM and long wavelength phase trend by GNSS velocity field (Tsai et al, 2015) following a conventional method (Fukushima and Hooper, 2011; Takada et al 2018), and stacked the six ascending interferograms. The descending interferogram was corrected in the same way. From these corrected interferograms, we derived the quasi-vertical and quasi-east velocity fields. Looking at the quasi-vertical component (Fig. 1), we found very rapid uplift up to 37 mm/yr with a gap in the uplift rate at the eastern flank of the uplift area. We also found a gap in the amount of uplift for coseismic interferogram of the Meinong earthquake (Mw 6.4) that occurred ~20 km east of the uplift area. We created coherence map for both interseismic (ALOS) and coseismic (ALOS2) interferograms (Fig. 2), and identified clear coherence loss along the eastern flank of the uplift area, which locates at the same location for both images. This coherence loss probably indicates a surface rupture due to a thrust faulting which keeps accumulating before and after the Meinong earthquake without seismicity.

Considering this thrust faulting, we constructed a two-dimensional fault model in an elastic half-space (Okada, 1992) and compared the numerical results with quasi-vertical (Fig. 3a) and quasi-east (Fig. 3b) velocity field for interseismic period. The optimum model has dip angle of 65 degree and slip rate of 55 mm/yr (Fig. 3c). This model well explains the quasi-east component, but there is remarkable misfit (15mm/yr) at the footwall side for the vertical component. In the plan view (Fig.1), it is clear that the footwall side (i.e., east) also uplifts, which strongly indicates that the newly found thrust fault only cuts shallow parts, and another driving force locates at deeper parts causing long wavelength uplift. In conclusion, we require the mud diapir at depth, as originally proposed by Ching et al. (2016), to explain the whole uplift pattern in addition to the surface offset. We further created interferograms after Meinong earthquake using ALOS2 images, and found that the uplift continues after the earthquake, which is consistent with mud diapirism considering that buoyancy and absolute stress should not change due to the earthquake.

References:

Tsukahara, K., and Takada, Y., Observation of aseismic crustal deformation in Taiwan by analysis of InSAR and GPS data. JPGU 2017

Takada, Y., Sagiya, T., Nishimura, T., Interseismic crustal deformation in and around the Atotsugawa fault system, central Japan, detected by InSAR and GNSS. Earth Planets and Space, accepted.

Acknowledgements:

PALSAR and PALSAR2 data were provided from PIXEL (PALSAR Interferometry Consortium to Study our Evolving Land surface) group under cooperative research contract between JAXA and ERI, University of Tokyo. PALSAR data were also provided from JAXA under ALOS2-PI project.

Keywords: InASR, GNSS, Taiwan

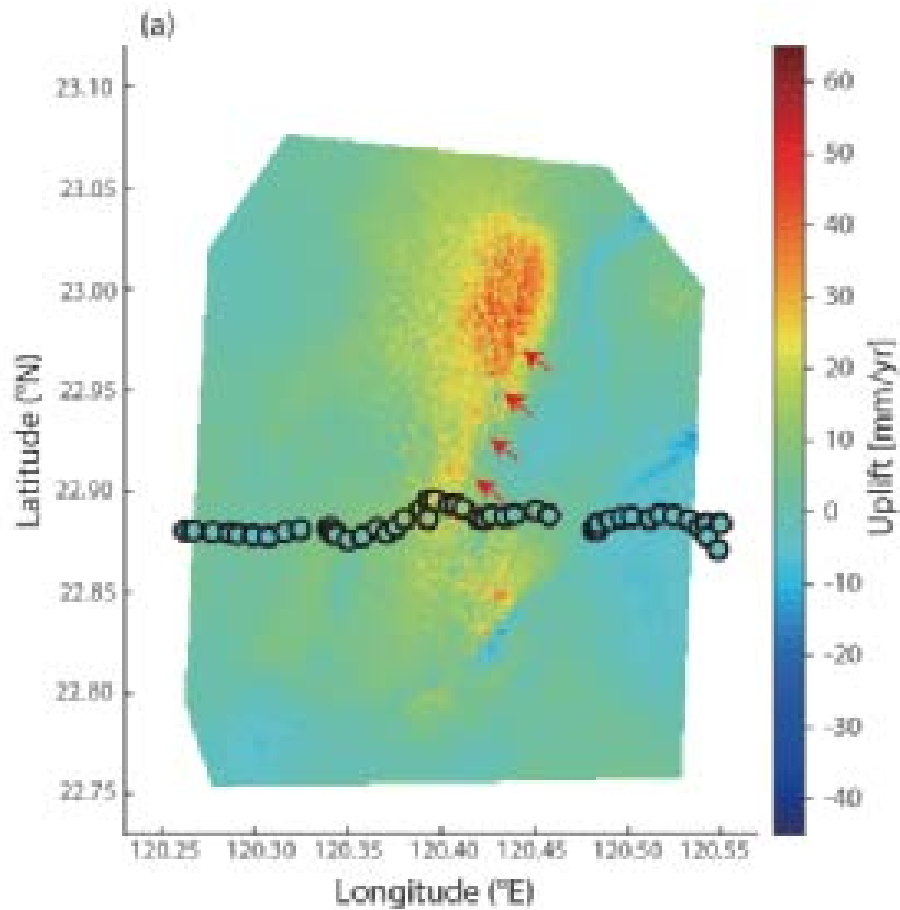


Fig.1 Quasi-vertical velocity field.

Red arrow indicates gap in the uplift rate.

Circles indicate leveling line of
Ching et al. (2016)

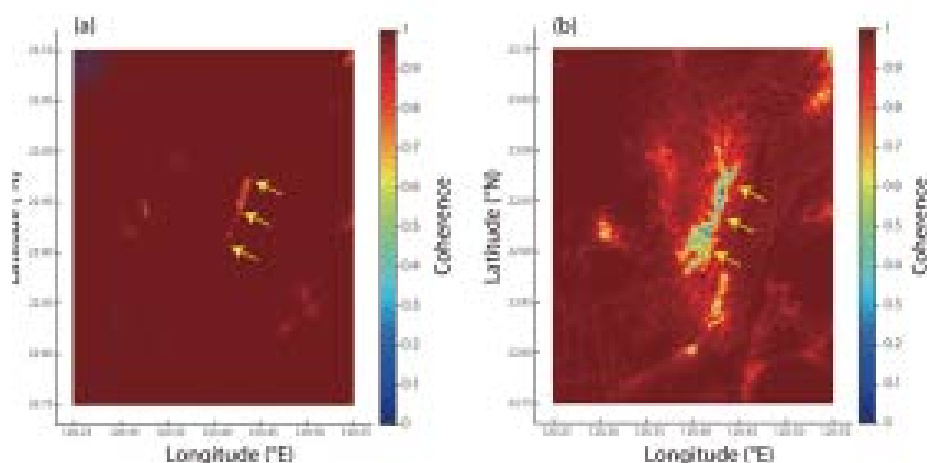


Fig.2 Coherence map of (a) coseismic and (b) interseismic interferograms.

Yellow arrows indicate coherence loss.

